ELSEVIER

Journal of Neuroscience Methods 90 (1999) 57–66

JOURNAL OF NEUROSCIENCE METHODS

# Examination of the spatial and temporal distribution of sensory cortical activity using a 100-electrode array

Patrick J. Rousche [a,*], Rasmus S. Petersen [b], Stefano Battiston [b], Sabina Giannotta [b], Mathew E. Diamond [b,c]

[a] *Optometry and Visual Science, University of Manchester Institute of Science and Technology, P.O. Box 88, M60 1QD Manchester, UK*
[b] *Cognitive Neuroscience Sector, International School for Advanced Studies, Via Beirut, 2–4, 34014 Trieste, Italy*
[c] *Department of Biomedical Sciences and Technologies, University of Udine, Via Gervasutta, 48, 33100 Udine, Italy*

Received 3 September 1998; received in revised form 15 April 1999; accepted 9 May 1999

**Abstract**

This paper introduces improved techniques for multichannel extracellular electrophysiological recordings of neurons distributed across a single layer of topographically mapped cortex. We describe the electrode array, the surgical implant techniques, and the procedures for data collection and analysis. Neural events are acquired through an array of 25 or 100 microelectrodes with a 400-μm inter-electrode spacing. One advantage of the new methodology is that implantation is achieved through transdural penetration, thereby reducing the disruption of the cortical tissue. The overall cortical territory sampled by the 25-electrode array is $1.6 \times 1.6$ mm (2.56 mm$^2$) and by the 100-electrode array $3.6 \times 3.6$ mm (12.96 mm$^2$). Using a recording system with 100 channels available, neural activity is simultaneously acquired on all electrodes, amplified, digitized, and stored on computer. In our data, average peak-to-peak signal/noise ratio was 11.5 and off-line waveform analysis typically allowed the separation of at least one well-discriminated single-unit per channel. The reported technique permits analysis of cortical function with high temporal and spatial resolution. We use the technique to create an 'image' of neural activity distributed across the whisker representation of rat somatosensory (barrel) cortex. 

*Keywords:* Spatial and temporal distribution; Sensory cortical activity; 100-Electrode array; Simultaneous multi-electrode recordings; Brain activity map

## 1. Introduction

With the realization that certain fundamental issues of neural coding can be addressed only by examining fine spatial and temporal patterns of distributed brain activity, neuroscientists have become increasingly interested in developing practical procedures to acquire such data. A wide range of methodologies is currently in use, each approach offering important capabilities together with technical limitations. Multiple wire recording arrays have allowed the chronic recording of multi-unit and single-unit neural activity in behaving animals for extended periods of time. For example, Nicolelis et al. (1997) have succeeded in obtaining neural data from limited areas of a single cortical area using single microwires arranged in a rectilinear fashion. However, the arrays span only two electrode rows (200 μM) in the transverse direction. In addition, the bundles or arrays cannot always be implanted with a precise, fixed geometric pattern, so that the exact spatial relationships among the recorded neurons cannot be determined. For studies of the hippocampus of behaving animals, McNaughton and colleagues have developed stereotrodes and tetrodes, which consist of intertwined microwires (Gray et al., 1995). These tools allow the investigator to efficiently discriminate the activity of single-units, but they are not ideally suited for sampling large regions in a precise pattern. Silicon-based microelectrode arrays, pioneered by Wise and Najafi (1991) represent a different and promising approach. The arrays are built using

*Abbreviations:* PSTH, peri-stimulus time histogram; S/N, signal to noise ratio; IP, intra-peritoneal; PSI, pounds per square inch.

* Corresponding author. Present address: Bioengineering Program, Arizona State University, ECG 202, Tempe, AZ 85287, USA. Tel.: +1-602-9654118; fax: +1-602-9650037.

*E-mail address:* rousche@asu.edu (P.J. Rousche)

0165-0270/99/$ - see front matter 
PII: S0165-0270(99)00061-8

2-D photolithographic techniques that allow the incorporation of integrated circuits directly onto the array. The arrays can sample from different depths with precise spacing in a cortical column, but to date it has not been practical to insert multiple electrodes to sample a horizontally distributed arrangement of neurons. Optical techniques have provided insights into how large areas of cerebral cortex process sensory information in vivo (Blasdel and Salama, 1986; Grinvald et al., 1986). However, optical imaging can only reveal spatially and temporally averaged neural activity in the superficial cortical layers, and the spatial resolution is usually far less than the single-neuron level in the cortex (Obaid et al., 1999). In addition, the requirement for an immobile recording apparatus in the vicinity of the exposed cortical surface represents a practical limitation.

Researchers from the University of Utah have developed an electrode array that appears to circumvent some of the limitations alluded to above (Jones et al., 1992; Rousche and Normann, 1992; Schmidt et al., 1993; Nordhausen et al., 1996; Rousche and Normann, 1998). The Utah array consists of 25 or 100 silicon microelectrodes geometrically arranged in a $5 \times 5$ or $10 \times 10$ grid-like pattern. Covering a territory of 2.56 or 12.96 $mm^2$, respectively, these arrays can span entire functional subdivisions of a single primary sensory cortical area in smaller mammals. In this report we present the current methodology for the simultaneous collection and analysis of 100 channels of neural signals acquired with the Utah array, as applied to the somatosensory 'barrel' cortex in rats. Barrel cortex has been studied intensively in recent years (Jones and Diamond, 1995) and the previous work with single-electrode methods provides fundamental data for comparison with our new data. The main advantage of the present method is its capacity to examine simultaneously the spike trains emitted by populations of neurons distributed across cortex with a known spatial arrangement. Surgical preparation time is equivalent to that of traditional single-electrode methods because electrodes can be implanted 'through' the dura, yet large groups of single-neurons can be recorded in parallel. Previous studies with this array have been limited by the number of simultaneous recordings or the number of available electrode connections (Nordhausen et al., 1996; Rousche and Normann, 1998). We demonstrate new experimental techniques that allow for the 'simultaneous' recording of 100 implanted electrodes and the creation of 'images' of cortical population or ensemble activity. The results suggest that this new methodology is particularly well-suited for the investigation of the functional organization of cerebral cortex.

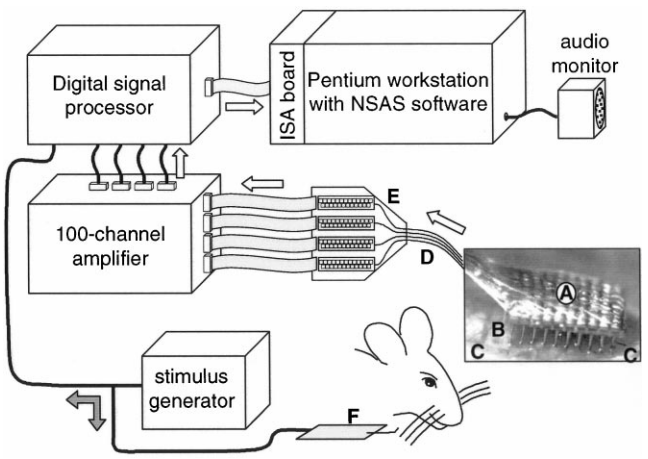


Fig. 1. Photomicrograph of an implanted electrode array together with a schematic representation of the additional components of the recording system. In the photograph, (A) is the back surface of the electrode array, (B) is the dura mater, and (C) is the bone. In the drawing, (D) is the 100-wire cable, (E) is the printed circuit interconnection board, and (F) is the whisker stimulator. The flow of neural information from the array to the Pentium workstation is indicated by the single arrows. The direction of pulses from the stimulus generator is indicated by the bifurcating arrows.

## 2. The components of the recording system

The entire recording apparatus is schematically illustrated in Fig. 1. The electrode array is micro-manufactured from a single block of silicon using a combination of mechanical sawing techniques and acid etching. Approximately 10–50 μm of exposed platinum at each tip provides a low impedance neural interface (120–300 kΩ measured at 1 kHz), while the remainder of the shaft is insulated with a 1-μm coating of silicon nitride. Electrodes are electrically isolated from each other with a glass dielectric which surrounds the base of each shaft. For complete details on electrode fabrication the reader is referred to Jones et al. (1992). For the experiments described in this report, two array configurations were used, either $5 \times 5$ (25 microelectrodes) or $10 \times 10$ (100 microelectrodes).

Electrodes are accessed by a Pt-Ir wire (25-μm diameter) bonded to the back of each electrode; all 25 or 100 electrode access wires are bundled together and potted with a silicone elastomer, forming a robust 6-cm cable (Fig. 1D) leading from the array to a printed circuit interconnection board (Fig. 1E). In addition, one wire placed under the skin of the contralateral hemisphere serves as a distant reference (not shown) and also leads to the circuit board. From the interconnection board, four, 40 cm, shielded ribbon cables (Fig. 1F), each carrying signals from 25 channels and the reference signal, lead to a 100-channel amplifier (Bionic Technologies, Salt Lake City, UT). The amplifier (gain = 5000, bandpass filtered from 250 to 7500 Hz) is connected to a digital signal processor (Bionic Technologies Inc.). The digitized signals (30 000 samples/s) are collected by an ISA interface board installed in the

Pentium PC, and are displayed and stored by data acquisition software (Bionic Technologies Inc.). Readers are referred to a complete description of the data acquisition and processing system elsewhere (Guillory and Normann, 1999). A threshold for unit event detection on each channel is manually or automatically set using the accompanying amplifier control software (Bionic Technologies Inc.). Upon threshold (typically two to three times greater than the RMS background noise) crossing on any given channel, the voltage values from 0.5 ms before threshold crossing until 1.0 ms following crossing are time-stamped and stored for off-line analysis. Raster plots of activity on all channels are viewed in real-time on a computer monitor; in addition, thresholded neural events for one selected channel are led to an audio monitor. Supplementary channels of the amplifier are available for analog inputs that are time-stamped and stored on hard disk in registration with neural events; in our case these inputs were used to record signals related to the delivery of mechanical stimuli to the whiskers.

## 3. Experimental procedures

### 3.1. Animal preparation and surgery

In the experiments used to illustrate the method, adult male Wistar ($n = 14$) or Lister Hooded rats ($n = 15$) weighing 250–400 g were used. Anesthesia was induced by urethane injection (1.5 g/kg of body weight, 30% aqueous solution, IP). During the recording session body temperature was maintained at 37–38°C and anesthetic depth was held at a consistent level by monitoring paw withdrawal reflex, heart rate, corneal reflex, and respiration rate. Supplemental doses of urethane (0.15 g/kg) were administered as necessary. With the animal in a stereotaxic frame, somatosensory cortex was exposed by a 7-mm diameter craniotomy centered on a point 2 mm posterior to Bregma and 6 mm from the midline. The dura was kept moist with saline. Some animals were sequentially implanted in both hemispheres with the same array. In the initial set of experiments, the array was implanted after removal of the dura. However, in later experiments the array was implanted through the dura, reducing surgery time and tissue trauma. Fig. 1 shows the transdural implantation of a $10 \times 10$ electrode array (Fig. 1A); the dura mater is intact (Fig. 1B) and the exposed bone forming the margin of the craniotomy is visible (Fig. 1C).

### 3.2. Positioning the electrode array

In general, electrode array positioning is a difficult and important stage of the experiment. Precise selection of the implant site is critical because removal of the array results in cortical trauma; subsequent reimplantation into the same hemisphere does not yield satisfactory results.

We used vascular landmarks, stereotaxic coordinates, and receptive field mapping with a single tungsten microelectrode (initial set of experiments only) to determine barrel cortex location prior to implant. In the implants for which we removed the dura, great care was taken to avoid prolonged pial exposure and manipulation before implant, as we found that inattention to pial hydration, or any pre-implant surface bleeding, could greatly decrease the probability of successful electrode recording after implantation. Once the implant site was determined, a wax membrane (Parafilm™) was stretched, and placed over the exposed region, to provide protection during array positioning. By applying saline to the Parafilm margin, the Parafilm adhered to the surface and became translucent. The entire electrode array and interconnection circuit board assembly were fixed in a manipulator with multiple degrees of freedom (Stoelting Scientific, Wood Dale, IL) and the array approximately placed on the target site. Before implant, the electrode tips must press lightly against the cortical surface at the target location with the shafts directed as normally as possible to the target site. A pair of #5 forceps, with tips protected by 1 mm-diameter polyethylene tubing, was used to provide fine adjustments of the cable which would adjust the position of the array. A pre-formed 'bend' in the cable a few millimeters from the array provided an excellent contact point for this task.

The array has very little mass in comparison to the to the wire cable or the attached printed circuit board; thus slight movements in the board or cable are often conveyed as large displacements of the array. Caution must be taken to prevent unwanted lateral or vertical array movement during the positioning. Contact of the array against the bone can break electrodes; shear movement of the array across the cortex can damage the dura mater or the pia itself and cause localized bleeding (when the protective membrane is not in place).

### 3.3. Inserting the electrode array

After the electrode array was appropriately placed, it was lifted gently by grasping the bend of the cable and slightly lifted 1–2 mm to allow removal of the Parafilm underneath with a second set of forceps. The array was then carefully placed directly onto the cortex in the target position. It was useful to view the positioned array from various angles to ensure that it was normal to the implant target and not in contact with any part of the bone. For implant, a pneumatic insertion tool (Bionics Technologies Inc.) was fixed in a second manipulator with multiple degrees of freedom. The inserter

tube (20 cm × 0.5 cm, roughly the size of a pencil) was arranged with its shaft closely perpendicular to the back of the array and then carefully lowered under observation through a dissecting microscope until it contacted the silicone elastomer insulation on the back surface of the array. Before starting the pneumatic pump, which causes vibration, the inserter tube was withdrawn about 50 μM, and subsequently lowered in place again for the implant. The pump air pressure setting of the pneumatic inserter can be regulated to control implant depth (for a full description see Rousche and Normann, 1992). For these experiments, a setting of 12 PSI was used to provide the full implantation depth of 1 mm. Higher implant pressures can cause the flat base of the array to press against the cortical surface. The amount of cortical curvature determines whether all electrodes will be inserted to a similar depth.

In some experiments, dural bleeding was observed immediately after implant. We treated this by simply applying warm saline until the bleeding stopped, and no negative effects on recording quality were noted. Subdural bleeding was rarely seen. A small piece of Parafilm was gently applied to cover the entire craniotomy and implanted array to maintain surface hydration for the duration of the experiment. A reference electrode wire (25 μm Pt-Ir) for differential recording was placed under the skin of the contralateral hemisphere. In our experience, typically 3 h elapsed between the start of surgery and the start of data acquisition. Overall 'yield' of recording success is difficult to assess. Many factors such as implant location, surgical technique, array condition and anaesthesia level can influence the recording results. Following a significant learning and training phase, our laboratories now post a roughly 50–75% success rate.

### 3.4. Removing and cleaning the electrode array

At the conclusion of the recording session, the array was removed by grasping the cable or the edge of the array itself using the #5 forceps sheathed by polyethylene tubing. Removal of the array nearly always caused bleeding and irreparable tissue damage. This precluded conclusive histological evaluation of implanted tissue in this study. Previous histological reports are available (Schmidt et al., 1993; Rousche and Normann, 1998). Explanted arrays were placed under a stream of warm saline within seconds of removal to avoid formation of blood clots on the electrodes. Any remaining blood clots were gently teased out under a dissection microscope using a fine camel hair artist's paint brush dampened with saline. In our experience a single array could be used in up to 20 experiments before the quality of recordings decreased (manifest by a reduced signal-to-noise ratio). Repeated handling inevitably leads to the breaking of some electrodes, usually those along the edge of the array, and shafts which are only partially broken should be removed at the base with a #5 forceps. This is to ensure that a broken electrode shaft does not induce tissue trauma during the next implant.

### 3.5. Vibrissal stimulation

Whiskers on the snout side contralateral to the array implant were trimmed to an even length (about 1 inch) and deflected, either individually or in sets. We used two methods for stimulation: (1) a hook, positioned just below the whisker shaft, 2 mm from the skin (Fig. 1F) and fixed to a piezoelectric ceramic bimorph wafer (Morgan Matroc, Bedford, OH); and (2) a lightweight aluminium lever, 3 inches in length, driven by a variable-speed motor. A stimulus generator (A.M.P.I., Jerusalem, Israel) delivered electrical pulses to the piezoelectric wafer (Fig. 1G) or provided a control signal to the motor which allowed for activation of the mechanical stimulus. Up-down step functions of 80 μm amplitude were induced 50 times for single whisker testing. Sinusoidal input waveforms provided a 90° deflection path of the lever which traversed a 2–3-inch arc for full whisker population stimulation. Full whisker stimulation was used to provide a quick and general assessment of exactly which electrodes were residing in the target barrel cortex.

## 4. Recording characteristics and cortical response images

### 4.1. Signal to noise ratio

Records of neural activity collected using a 5 × 5 array are shown in Fig. 2. Only ten channels (randomly chosen from the 25 total) are shown for clarity. A set of whiskers was deflected with the stimulus waveform shown at the bottom, and evoked activity is evident along many channels. The S/N ratio (defined as the peak-to-peak voltage values of the largest recorded action potential divided by the mean peak-to-peak voltage values in the absence of any action potential) is a useful measure of recording quality. In the illustrated data, the S/N ratio on different channels ranges from 6 to 13. In six experiments conducted with this 5 × 5 electrode array we calculated the average S/N ratio for a 3 × 3 block of electrodes at the center of the array (to avoid possibly broken edge electrodes). Data were obtained during controlled whisker stimulation. Among the nine electrodes of interest over all sessions, the average S/N ratio was 11.5 (standard deviation = 1.1) as shown in Table 1.

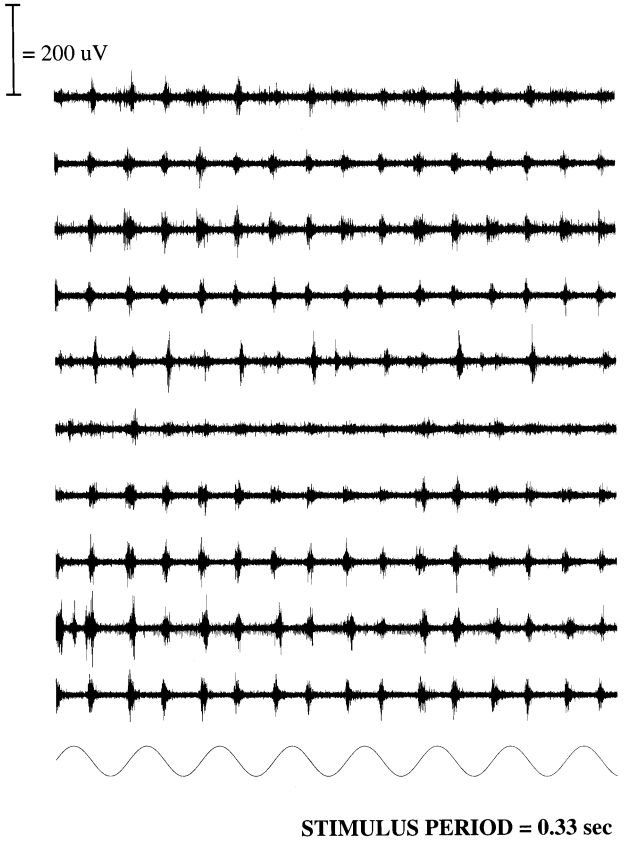


Fig. 2. Sensory responses recorded simultaneously at ten barrel cortex sites during sinusoidal stimulation of all whiskers. The bottom trace indicates upward and downward deflection patterns of the stimulator. Maximum signal amplitudes are roughly 150 μVolts.

### 4.2. Single-neuron discrimination

Some physiological studies require discrimination of single-neuron events. For example, quantitative measures of information transmission (Rieke, et al., 1996; Rolls and Treves, 1998) depend upon a set of single-neuron responses as a function of stimuli. However, 'cluster' recordings of several single units per electrode can also contain significant information (South and Weinberger, 1995). In this light, it was important to determine whether the recording system permitted single-unit discrimination versus multi-unit 'cluster' classification. To show the characteristics of recorded waveforms, Fig. 3 shows data acquired from a single electrode in the array at progressively higher temporal resolution (the data were recorded without using a voltage threshold in order to collect a 'continuous' trace). The largest discriminable single unit in this cluster of action potentials exhibited a S/N ratio of approximately 13.

Table 1
Average S/N for nine central electrodes over six different recording experiments[a]

| | |
|---|---|
| Session 1 | $10.9 \pm 2.5$ |
| Session 2 | $12.6 \pm 2.0$ |
| Session 3 | $9.9 \pm 2.4$ |
| Session 4 | $11.9 \pm 3.5$ |
| Session 5 | $12.7 \pm 2.6$ |
| Session 6 | $11.0 \pm 2.4$ |
| Total | $11.5 \pm 1.1$ |

[a] Sample maximum = 16.6; sample minimum = 7.1.

On each channel spikes exceeding a voltage threshold chosen on-line were stored on the PC hard disk as a digitized waveform. The set of neurons on any given channel whose action potentials exceed the threshold is referred to as the 'neural cluster' for that channel. Fig. 4(A) shows the action potential waveforms for one neural cluster, with all spikes aligned at the minimum peak value following threshold crossing. Discrimination between the action potentials of the neurons in the cluster was performed off-line using custom, in-house software implemented in Matlab (Mathworks, Natwick, MA); an outline of the method is given here. Several quantities of each waveform are analytically determined (Fig. 4B): the amplitudes *h1*, *h2* and *h3* of the phases of the waveform, the duration *w* of the negative phase at half-amplitude, and the areas under the waveform *I1*, *I2*, *I3* as indicated by shading. For each action potential recorded on the channel, the measured values for these parameters are then plotted in a series of graphs, with one graph for each pair of parameters. The experimenter selects the pair of parameters that best separates the different waveform shapes in the neural cluster—for the illustrated channel the plot of *h3* against *w* is selected (Fig. 4C). The experimenter can choose to view the data as a scatter plot or as a density plot, shown here. Discriminable waveforms tend to group into separable 'galaxies' or 'clusters' within the plot. On this plot, the experimenter traces lines around the areas of highest density to separate groups of waveforms clustered together according to the two parameters. In this case, two lines (dotted) have been traced around two central high-density zones (Fig. 4C).

It is useful to consider all of the individual spike waveforms as vectors with *i* elements (the number of time samples per waveform). For each selected group of waveforms, the program generates an initial 'template' waveform, the mean vector of the group. Each recorded waveform is then assigned to the 'nearest' template. Nearness is given by Eq. (1):

$$d(W^{s},\ T^{K}) = \left(\sum_i (W_i^{s} - T_i^{K})^2\right)^{1/2} \quad (1)$$

where $d(W^{s}, T^{K})$ is the Euclidean distance between the spike waveform vector $W^{s}$ and the $K^{th}$ template, $T^{K}$. After all spike waveforms have been assigned to the nearest template, new mean waveforms are computed from all the spikes assigned to a given template. A 'confidence tube' is then generated around each mean

template shape, consisting of the template $\pm 2$ standard deviations for each point along the waveform. In Fig. 4(D) the gray waveforms fall within the confidence tube (lighter dotted lines, not fully visible due to overlap) of the template originating in the top left cluster of Fig. 4(C). The black waveforms fall within the confidence tube (black dotted lines) of the template originating in the lower right cluster of Fig. 4(C). Warnings are provided if the interspike interval is less than a value selected by the user. Finally, the user has the option of concluding the selection by 'rejecting' spikes by subjective criteria. A complete description of the statistics of this algorithm is beyond the scope of this report (however, see Fee et al. (1996), and Lewicki (1994) for a description of statistical validation of sorted waveforms).

The outcome of this spike-sorting procedure is shown for 20 adjacent channels in a $5 \times 5$ array (Fig. 4E). Channels 1, 2, 5, 7, and 8 yielded two discriminable waveforms each (marked with an asterisk), while other channels yielded one discriminable waveform (channel 8 is illustrated in Fig. 4A–D).

### 4.3. Response properties

Somatosensory 'barrel' cortex of rodents has been intensively studied with single-electrode methodology since the 1970s (Woolsey and Van der Loos, 1970; Ito, 1985; Diamond et al., 1993). To evaluate whether neuronal functional properties were affected by the large recording array, we asked whether the neurons recorded with the present methodology exhibited response properties similar to those reported with single-electrode techniques. The most common analysis tool of neural response properties is the peri-stimulus time histogram or PSTH. Therefore, we formed PSTHs (bin size of 5 ms) from the activity of single-unit or neural 'clusters' during whisker deflection. A typical example is given in Fig. 5. The stimulus was an up–down step function of 80 μm amplitude and 100 ms duration, delivered to each of two whiskers 50 times at 1 Hz. Activity was recorded from two neighboring electrodes ( # 56 and # 57) in a $10 \times 10$ array during stimulation, separately, of whiskers $D_1$ and $D_2$. The neurons at each electrode gave a strong, short-latency response to their 'principal' whisker and a weaker, long-latency response to the adjacent whisker. In general, the spontaneous activity and sensory response properties of the neurons recorded with any individual electrode within a $5 \times 5$ or $10 \times 10$ array were not distinguishable from those of neurons recorded with a single-electrode under the same conditions of anesthesia. Our conclusion is that the present methodology yields data in which cortical neurons have normal functional characteristics.

### 4.4. Cortical activity maps

With the array inserted in sensory cortex, it is possible to record simultaneously from 100 channels to generate stimulus-evoked neural activity maps. In Fig.

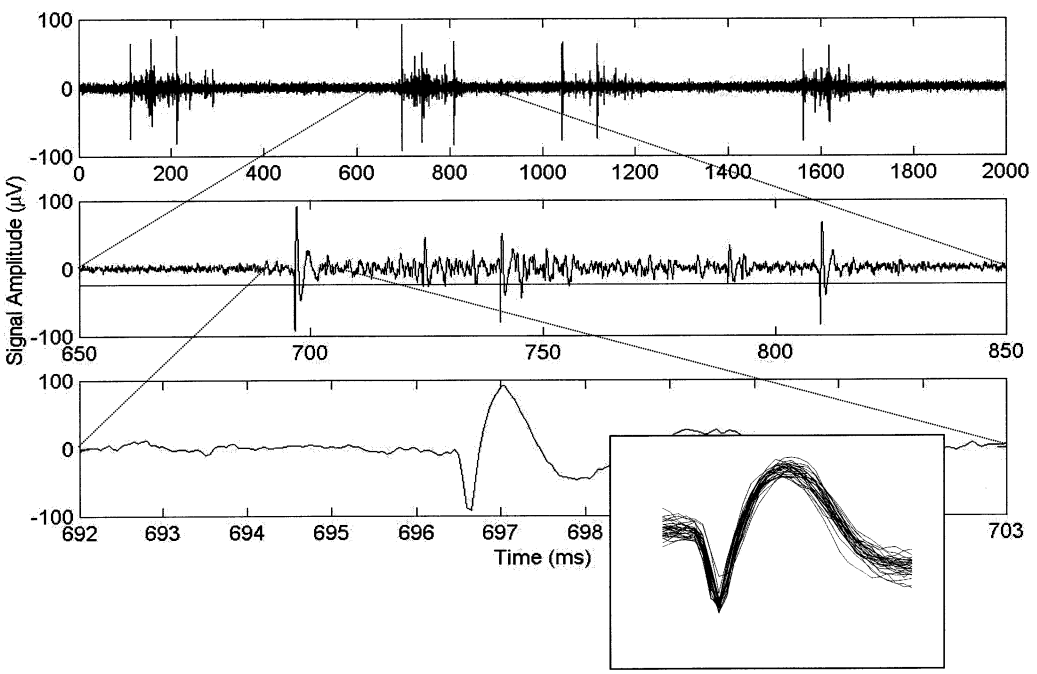


Fig. 3. Discrimination of single-unit activity. A trace of recorded activity is illustrated at increasing temporal magnification. The inset in the lower plot shows a single unit event waveform isolated by spike-sorting algorithms. Although several units are located within the firing cluster, only the largest unit is separated. S/N of this unit is about 13, slightly higher than the population sample of 11.5 described in Table 1.

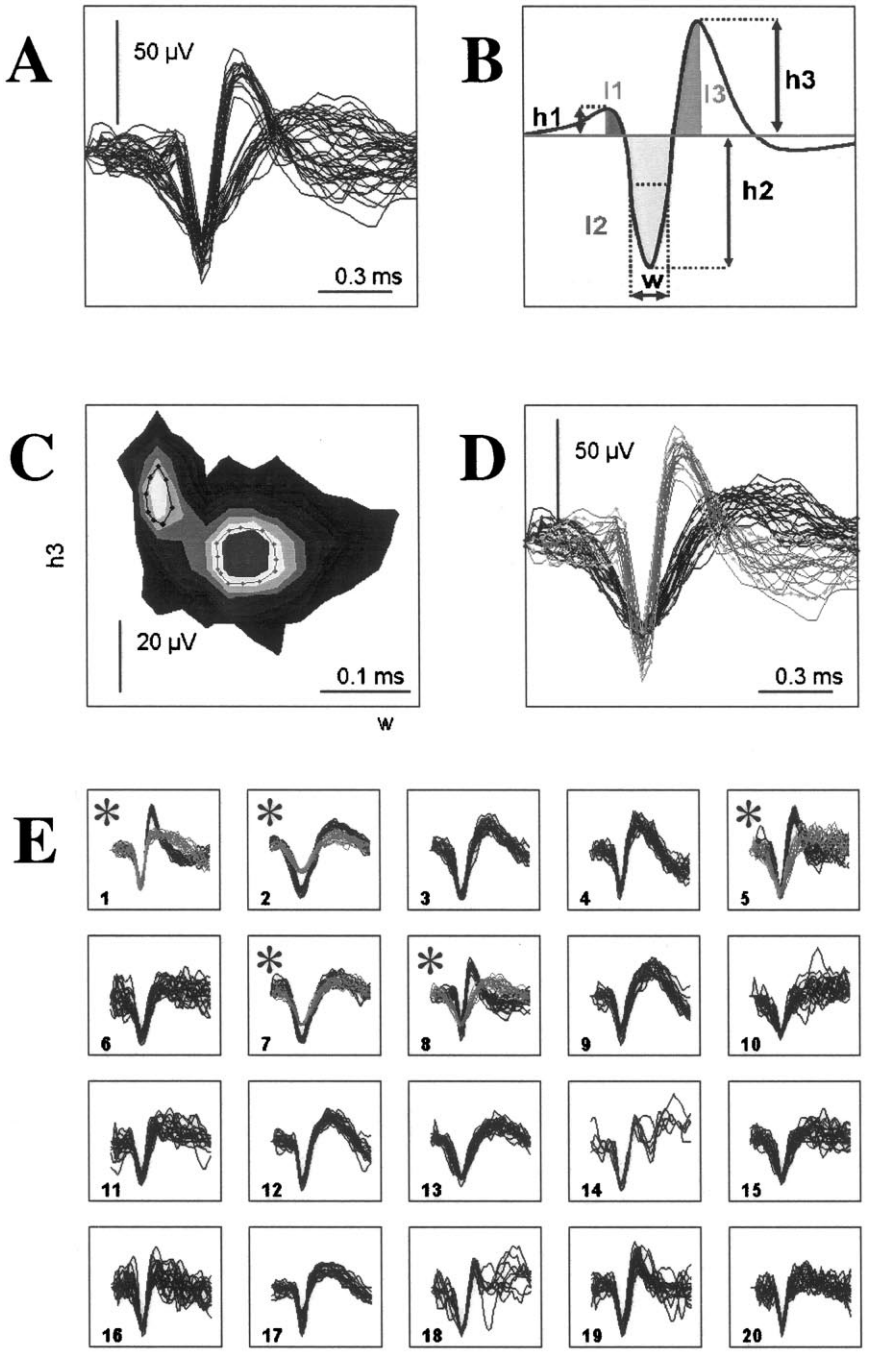


Fig. 4. Spike separation for a single array. (A) Collected action potential waveforms which have crossed threshold for one neural cluster from one electrode. (B) Waveform features used in the single unit clustering algorithm (see text). (C) Density plot for a pair of waveform features (phase 2 width vs. phase 3 amplitude), user input is required to define separable clusters (two are traced with dotted lines). (D) Classification results. Gray (lighter) waveforms fall within the confidence tube (gray dotted lines) of the template originating in the top left cluster of (C), while the black waveforms fall within the confidence tube (dark dotted lines) of the template originating in the lower right cluster of (C). (E) Sorted spikes for 20 adjacent channels in a $5 \times 5$ array. Several channels have multiple units shown in gray and in black (marked with an asterisk).

6, two such maps are shown. The array was positioned in the vibrissal region of somatosensory cortex; the stimulus was repetitive deflection of four vibrissae together, E1–E4. The data are first illustrated as a $10 \times 10$ grid of PSTHs (bin size 5 ms) constructed in parallel across all channels (Fig. 6A). The temporal aspect of the response is apparent in the distribution of events across the individual histograms. For example, note that the PSTHs with the most abrupt onset of response also possess the largest magnitude of response. The same data are replotted below in grayscale to emphasize the spatial arrangement of the cortical response

map (Fig. 6B). Response values per trial for this image are taken from the entire 40 ms interval of the PSTHs. This population activity image is comparable to what might be derived by optical imaging. However, with the present methodology the individual neurons making up the population can be further investigated on a ms time scale.

## 5. Discussion

This paper illustrates a method for simultaneous recording of cortical neuronal activity using an array of 25 or 100 microelectrodes geometrically arranged with equal spacing. Over numerous implants, we have developed a technique which provides precise spatial and temporal neuronal firing information in the rat barrel cortex. In this section we discuss the limitations and capabilities of this technique as well as its significance.

### *5.1. Limitations and capabilities*

The method presented here has certain properties which limit the research problems to which it can be applied. The electrodes advance together and cannot be controlled independently. In addition, although the arrays are ideal for studying cerebral cortex and other tissues lying at or near the brain surface, in the configuration currently available the electrode tips cannot reach structures located deeper than 1.5 mm.

Several advantageous features of the experimental method are noteworthy. The surgical procedure is simple. The dura mater may be left intact, protecting the underlying cortex. Transdural impulse insertion of the array appears to produce very little cortical damage in most experiments, judging from the absence of edema or bleeding. This development is notable for researchers who are interested in long-duration acute procedures. Recorded neuronal activity may be analyzed as single-units or as neuronal clusters depending on the question to be addressed. In either case, the functional characteristics of the recorded neurons, as judged by their sensory response characteristics (PSTHs in Fig. 5), are identical to those previously reported in single-electrode studies.

Pilot studies with chronic implants of this type of array demonstrate that the neural tissue adjacent to the normal neural tissue can co-exist in close proximity to an implanted array (Schmidt et al., 1993; Rousche and Normann, 1998). In the few cases when surface bleeding does occur upon implant, the bleeding is resolved quite quickly and does not seem to compromise the underlying cortical tissue in any way. Thus, we suggest that these experiments are equivalent to the implantation of 100 single electrodes, which individually do not cause significant tissue disruption.

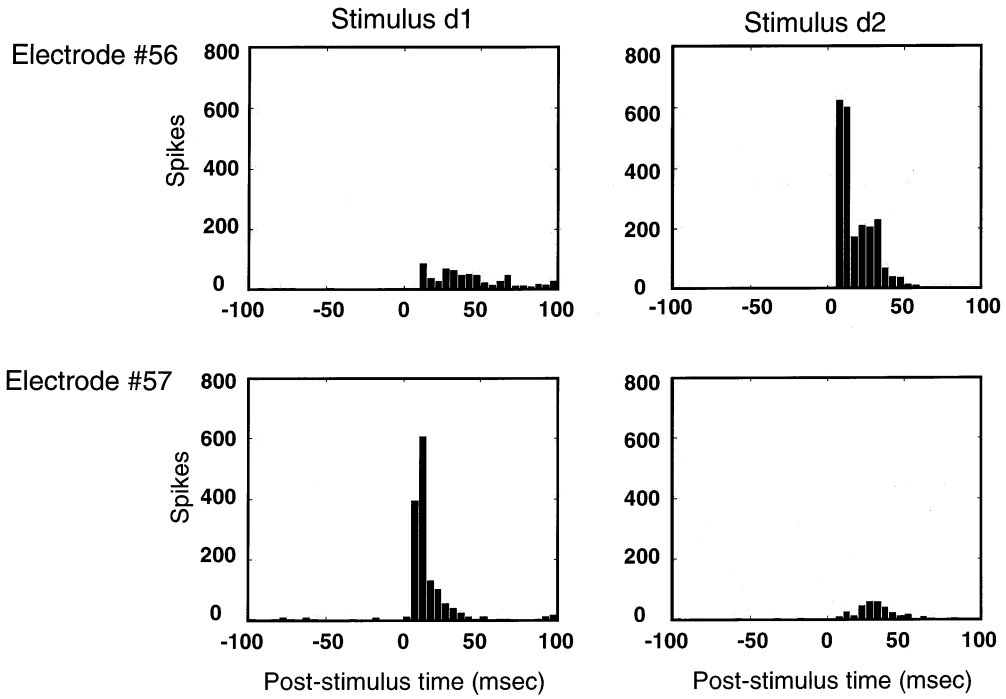


Fig. 5. Functional responses for two different electrodes. PSTHs for single whisker stimulation obtained from two neighboring electrodes (top row and bottom row). Stimulation of vibrissae D1 (left column) preferentially activates electrode # 57. Stimulation of vibrissae D2 (right column) does not activate electrode # 57, but does produce a strong response on the neighbor, electrode # 56. Thus the neighboring electrodes (400 μm separation) reside in separate barrels.

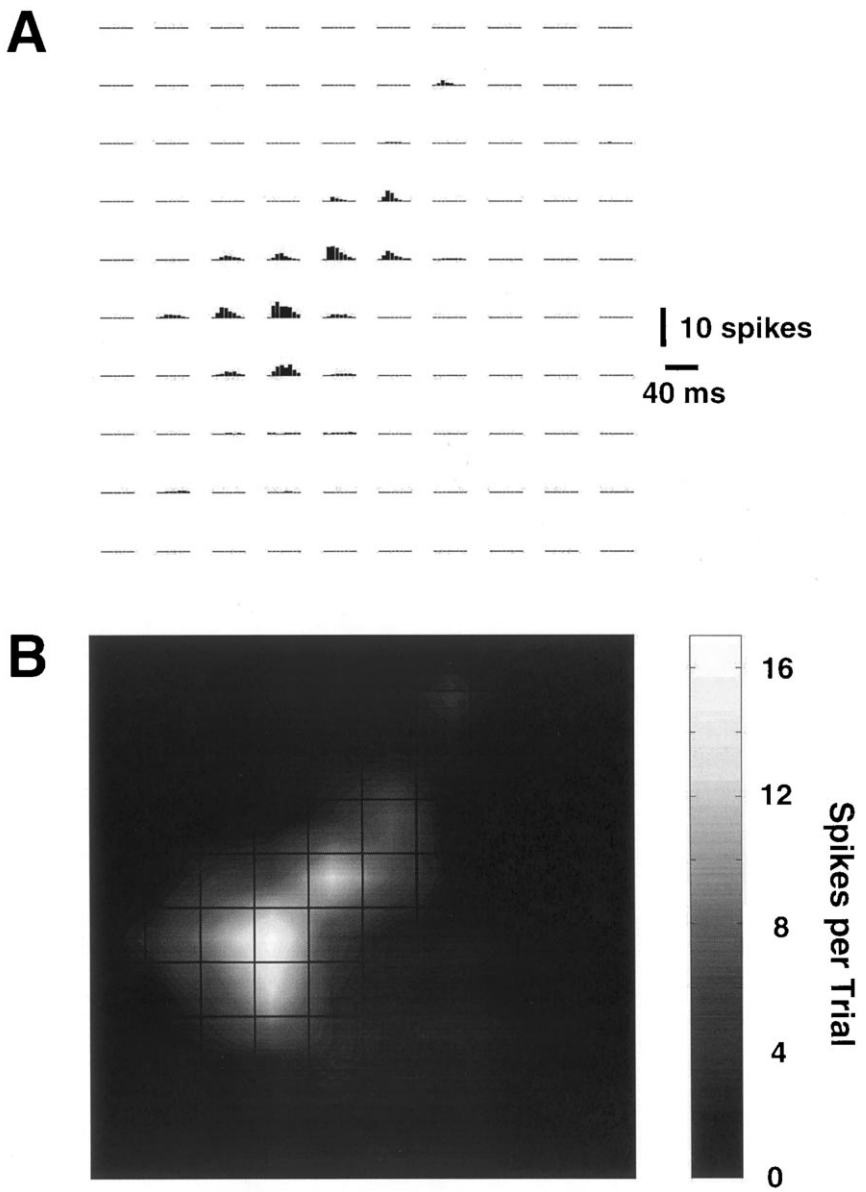


Fig. 6. Reconstructed images of whisker-evoked cortical activity. The data are arranged to represent the $10 \times 10$ matrix of electrodes covering a $3.6 \times 3.6$ mm field of cortex. (A) PSTH onset corresponds to the beginning of vibrissal deflection (four whiskers—E1–E4). Response values are in events per trial. Twenty-two of the 100 electrodes show some type of response. (B) The data in the PSTHs have been interpolated across electrodes to form a cortical response map. Cortical response reflects the linear arrangement of stimulated whiskers E1–E4 in a transverse strip of activity from lower left to upper right.

### *5.2. The significance of parallel recordings from a geometrically arranged array*

Acquisition of spike trains from multiple neurons is of fundamental importance because the information present within the activity of a neuronal ensemble cannot always be predicted if the single-neuron activities making up the ensemble are considered independently. For example, in auditory cortex information about the tonic phase of a tone stimulus is present not in single neuron activity but in multi-neuron correlations (deCharms and Merzenich, 1996). In frontal cortex information about the upcoming motor response is sometimes carried not by single neurons but by the precise temporal firing relationships within a neuronal ensemble (Vaadia et al., 1995).

In sensory cortex, information is represented not only by a temporal code but also by a topographic code: some parameters of stimulus space (e.g. retinal position, sound wave frequency, or location on the body surface) are distributed in a regular way across the cortical territory (Kaas, 1997). In other words, sensory cortex represents external events both by the temporal relationships between spike trains and by the spatial relationships between neurons. The amount of information available to the investigator regarding cortical processing of sensory stimuli is thus maximized if both types of relationships, temporal and spatial, are conserved during the physiological recording session.

In that light, the principal strength of the new method is the juxtaposition of temporal relationships among neuronal spike trains and the spatial relationships among the neurons emitting the spike trains (Harris et al., 1999). Such relationships can only be reliably obtained with a large number of microelectrodes through the 'simultaneous' collection of neural data. In this report, the distance between adjacent electrode tips is 400 μm, equivalent to the diameter of a cortical 'macrocolumn' (Favorov and Diamond, 1990). Using the $10 \times 10$ arrays, each cortical column within a territory of almost 13 $mm^2$ is sampled by at least one microelectrode. The activity maps in Fig. 6, representing the distribution of evoked activity across 100 electrodes, demonstrate that 'images' of brain activity can be generated at high temporal and spatial resolution using an efficient simultaneous recording technique.

## Acknowledgements

Supported by the Whitehall Foundation, NSF grant IBN 94-24509, NIH grant NS32647, Telethon Foundation grant 984, and the Italian MURST. We thank G. Mirabella and I. Erchova for participating in some experiments. We thank Richard A. Normann for experimental support and for reviewing this manuscript.

## References

Blasdel GG, Salama G. Voltage-sensitive dyes reveal a modular organization in monkey striate cortex. Nature 1986;321:579–85.

deCharms RC, Merzenich MM. Primary cortical representation of sounds by the coordination of action-potential timing. Nature 1996;381:610–3.

Diamond ME, Armstrong-James MA, Ebner FF. Experience-dependent plasticity in the barrel cortex of adult rats. Proc Natl Acad Sci USA 1993;90:2602–6.

Favorov OV, Diamond ME. Demonstration of discrete place-defined columns 'segrates' in the cat SI. J Comp Neurol 1990;298(1):97–112.

Fee MS, Mitra PP, Kleinfeld D. Variability of extracellular spike waveforms of cortical neurons. J Neurophysiol 1996;76(6):3823–33.

Gray CM, Maldonado PE, Wilson M, McNaughton B. Tetrodes markedly improve the reliability and yield of multiple single-unit isolation from multi-unit recordings in cat striate cortex. J Neurosci Methods 1995;63:43–54.

Grinvald ALE, Frostig RD, Gilbert CD, Wiesel TN. Functional architecture of cortex revealed by optical imaging of intrinsic signals. Nature 1986;324:361–4.

Guillory S, Normann RA. A 100-channel system for aquisition and storage of extracellular spike waveforms. J Neurosci Methods 1999 (in press).

Harris JA, Petersen RS, Diamond ME. Distribution of tactile learning and its neural basis. Proc Natl Acad Sci USA 1999;96(13):7587–91.

Ito M. Processing of vibrissa sensory information within the rat neocortex. J Neurophysiol 1985;54:479–90.

Jones EG, Diamond IT. Cerebral Cortex, Vol. 11: Barrel Cortex. New York: Plenum Press, 1995.

Jones KE, Campbell PK, Normann RA. A glass/silicon composite intracortical array. Ann Biomed Eng 1992;20:423–37.

Kaas JH. Topographic maps are fundamental to sensory processing. Brain Res Bull 1997;44:107–12.

Lewicki M. Bayesian modeling and classification of neural signals. Neural Comput 1994;6(5):1005–30.

Nicolelis MA, Ghazanfar AA, Faggin BM, Votaw S, Oliveira LM. Reconstructing the engram: simultaneous, multisite, many single neuron recordings. Neuron 1997;18(4):529–37.

Nordhausen CT, Maynard EM, Normann RA. Single unit recording capabilities of a 100 microelectrode array. Brain Res 1996;726:129–40.

Obaid AL, Koyano T, Lindstrom J, Sakai T, Salzberg BM. Spatiotemporal patterns of activity in an intact mammalian network with single-cell resolution: optical studies of nicotinic activity in an enteric plexus. J Neurosci 1999;19:3073–93.

Rieke F, Warland D, de Ruyter van Steveninck RR, Bialek W. Spikes: Exploring the Neural Code. Cambridge, MA: MIT Press, 1996.

Rolls E, Treves A. Neural Networks in the Brain. Oxford: Oxford University Press, 1998.

Rousche PJ, Normann RA. A method for pneumatically inserting an array of penetrating electrodes into cortical tissue. Ann Biomed Eng 1992;20:413–22.

Rousche PJ, Normann RA. Chronic recordings in cat sensory cortex using the Utah Intracortical Electrode Array. J Neurosci Methods 1998;82(1):1–15.

Schmidt S, Horch K, Normann RA. Biocompatibility of silicon based electrode arrays implanted in feline cortical tissue. J Biomed Mater Res 1993;27:1393–9.

South DA, Weinberger NM. A comparison of tone-evoked response properties of 'cluster' recordings and their constituent single cells in the auditory cortex. Brain Res 1995;704(2):275–88.

Vaadia E, Haalman I, Abeles M, Bergman H, Prut Y, Slovin H, Aertsen A. Dynamics of neuronal interactions in monkey cortex in relation to behavioural events. Nature 1995;373:515–8.

Wise KD, Najafi K. Microfabrication techniques for integrated sensors and microsystems. Science 1991;254:1335–42.

Woolsey TA, Van der Loos H. The structural organization of layer IV in the somatosensory region (SI) of mouse cerebral cortex. The description of a cortical field composed of discrete cytoarchitectonic units. Brain Res 1970;17:205–42.